Photofission of ^{238}U with neutron-capture gamma rays

Sylvian Kahane and Alex Wolf
Physics Department, Nuclear Research Centre-Negev, Beer-Sheva, Israel
(Received 20 May 1985)

Fission yields from the photofission of ^{238}U with neutron capture γ rays were measured at an effective excitation energy $E_x = 7.8$ MeV. The mass distribution of the fission fragments was deduced by measuring yields of 19 mass chains with respect to ^{135}Xe, whose cumulative yield was measured directly. The results are in general agreement with those obtained by Jacobs *et al.* using bremsstrahlung at higher energies. However, a systematic decrease of the yields of a few mass chains was observed. This decrease can be attributed to a change in the shape of the light and heavy mass distributions, as a function of energy. The ratio Γ_n/Γ_f was measured at two energies and its values confirm recent theories on the shape and height of the second fission barrier in ^{238}U. The most probable charge Z_p was obtained for the mass chains 92, 134, and 135 at three energies.

I. INTRODUCTION

Most of the recent work on the photofission of ^{238}U was done with bremsstrahlung beams providing effective energies higher than 10 MeV.[1-3] The fission process is clearly more interesting at lower energies, closer to the fission threshold, where only a limited number of fission channels are open.

A number of experiments were performed with highly monoenergetic neutron capture γ rays. These beams provide a small number of relatively intense γ lines under 10 MeV. Manfredini *et al.*[4] and Mafra *et al.*[5] used them mainly for cross-section measurement. Mafra also reported measurements of the ratio Γ_n/Γ_f, an important parameter in the fission process.

In the present work, neutron capture γ rays from the Fe(n,γ), Ni(n,γ), and Cr(n,γ) reactions, were used to study mass distribution, fractional cumulative yields, and Γ_n/Γ_f ratios for photofission of ^{238}U. The mass distribution reported in this work, at an effective excitation energy of 7.8 MeV, is at the lowest energy measured so far for the fission of the ^{238}U nucleus.

A comparison of our results with mass distributions at higher excitation energies indicates the existence of a change in the asymmetry of the light and heavy fragments distributions as a function of energy. For three mass chains, most probable charges Z_p were obtained at three excitation energies, and compared with empirical formulae compiled from data on thermal neutron fission of ^{233}U and ^{235}U. The measured Γ_n/Γ_f ratios, at excitation energies of 7.8 and 9.0 MeV, support the assumption of a complex second barrier in the fission of the ^{238}U nucleus.

II. THE EXPERIMENTAL METHOD

Incoming γ beams were produced by (n,γ) reactions on separate metallic disks of Fe, Cr, and Ni, placed near the core of the reactor in tangential beam tubes. After collimation and neutron filtration the intensities of the γ beams on the target position were of the order 10^6 photons/cm^2 sec. There are a small number of monoenergetic γ lines, in each of the incoming beams, above the photofission threshold. Taking in consideration the intensities[6] of these γ lines, and the fission cross section,[7] effective excitation energies have been calculated for three (n,γ) sources (Table I). These energies are already quite far from the threshold and no exotic angular distributions are expected for the fission fragments. They are still lower than the recent bremsstrahlung work[1] and, by comparison, trends in energy could be established.

A new technique is introduced for measuring cumulative yields absolutely, with no need of renormalizing the mass distribution to 200%. Avoiding the renormalization means that there is no need for inferring results at the mass chains not measured, and a source of systematic errors is thus eliminated. The technique consists of two steps: in the first one absolute determination of the ^{135}Xe yield is done and, in the second step, relative yields are measured with respect to ^{135}Xe for the other isotopes.

For the first step the fission yield is measured with solid state detectors from a thin evaporated target, and the intensity of the ^{135}Xe 249 keV γ line is measured from a second target of similar geometrical dimensions, with a Ge(Li) detector after irradiation. Keeping the geometry

TABLE I. List of principal gamma lines, relative intensities, and effective excitation energies of ^{238}U, for the three (n,γ) sources used in this experiment.

Source	γ line	Relative intensity	E_x (MeV)
Fe(n,γ)	7.279 MeV	4.6	
	7.632 MeV	27.2	7.8 MeV
	7.646 MeV	22.1	
	9.298 MeV	3.8	
Cr(n,γ)	7.939 MeV	11.4	
	8.884 MeV	24.1	8.8 MeV
	9.720 MeV	9.8	
Ni(n,γ)	7.819 MeV	9.0	
	8.533 MeV	18.7	9.0 MeV
	9.000 MeV	41.7	

 ©1985 The American Physical Society

the same ensures that any structure in the incoming γ-beam profile will not influence the results. In the second step a large U_3O_8 target is irradiated and a wealth of γ lines from various isotopes are detected and measured.

In addition to the fragments mass distribution measured at 7.8 MeV, evaluation of the most probable charge Z_p, and of the ratio Γ_n/Γ_f was done in a small number of cases as a function of energy.

We shall present a detailed description of the mass distribution measurement in two parts. Section III is devoted to the absolute measurement of the ^{135}Xe yield, and Sec. IV to the relative measurement of other isotopes yields. In Secs. V and VI a description of the fractional cumulative yields and Γ_n/Γ_f ratios is given. These measurements are simple variations on the technique employed for the mass distribution evaluation.

III. ABSOLUTE CUMULATIVE YIELD OF ^{135}Xe

In order to calibrate the mass distribution measurements, it was necessary to obtain an absolute yield for one of the mass chains. The main difficulty in obtaining such an absolute value, consists in its dependence on $\sigma(\gamma,f)$—the photofission cross section—and on I_γ—the absolute intensity of the incoming photon beam—both not known very well. The following method was devised in order to overcome the use of I_γ and $\sigma(\gamma,f)$:

(a) The fission yield N_f of a thin evaporated (1.25 cm diameter) ^{238}U target was measured with a solid state detector

$$N_f = 2n_1\sigma(\gamma,f)I_\gamma f_1 t_f \Omega/4\pi(1+a_2P_2+a_4P_4)\ , \qquad (1)$$

where n_1 is the number of ^{238}U atoms in the target, f_1 is a factor correcting for the reactor power fluctuations, t_f is the time of the measurement, Ω is the solid angle of the detector, and a_2, a_4 are angular distribution coefficients of the ejected fission fragments.

(b) The gamma yield N_γ of the 249 keV line of ^{135}Xe, following the γ irradiation of a second target (1.25 cm diameter) of depleted (0.04% ^{235}U) uranium, was measured with a Ge(Li) detector:

$$N_\gamma = n_2 I_\gamma \sigma(\gamma,f)\epsilon f_2 B_0 g f_p(T,t_1,t_2)C^c_{135}\ , \qquad (2)$$

where n_2 is the number of nuclei in the second target, f_2 is the reactor power correction factor, ϵ is the absolute Ge(Li) detector efficiency at 249 keV, B_0 is the branching ratio for the 249 keV γ ray of ^{135}Xe, g is the correction factor for self-absorption in the target, C^c_{135} is the absolute cumulative yield of ^{135}Xe, and f_p is a function expressing parent-daughter relations in a decay chain, defined in Eq. (6) (see below).

The above expression contains two slight approximations. First, the contribution of a metastable state at 526.5 keV in ^{135}Xe, to the population of the ground state, is neglected [see discussion after Eq. (11)]. Second, in place of C^c_{135} one has to write $C^c_p + C^i_d f_d/f_p$; C^c_p being the cumulative yield of ^{135}I, and C^i_d the independent yield of ^{135}Xe [see Eqs. (6)–(10) and the discussion therein]. The ratio f_d/f_p depends on the decay constants, irradiation, and accumulation times, and in our case was 0.955. Since C^i_d is of the order of 4% of C^c_p,[8] we used the approximation

$$C^c_p + C^i_d f_d/f_p \sim C^c_p + C^i_d = C^c_{135}$$

which is obviously valid when $C^i_d \ll C^c_p$ and f_d/f_p is close to 1.00.

Taking the ratio of Eq. (2) to Eq. (1) we get:

$$N_\gamma/N_f = C^c_{135}[n_2\epsilon B_0 g f_2 f_p]/[2n_1 t_f f_1 \Omega/4\pi(1+a_2P_2+a_4P_4)]\ . \qquad (3)$$

Two independent measurements were performed in order to determine all the quantities entering in expression (3), as described below.

A. Fission fragments measurement

Fission yields were measured at 13 angles with a solid state fission detector of 400 mm^2 area and 60 μ depletion layer. The target was a ^{238}U film of 1.25 cm diameter, evaporated on a glass backing. The target thickness was determined by alpha counting, and found to be 394 μg/cm^2. The target-detector distance was 4.8 cm. The target was placed in the incoming γ beam from a Fe(n,γ) source located near the core of the Israel Research Reactor-2 (IRR-2) reactor. The statistical error of each measurement was around 5%. The contribution of the fast and thermal neutron fission, in addition to the photofission, was estimated to be less than 2% by placing a 1 cm thick Ta absorber in the γ beam. The fission yield was reduced (within $\pm$2%) by the attenuation factor of the γ beam in the Ta absorber. The angular distribution is presented in Fig. 1. It was not possible to extract a reliable a_4 coefficient and only a_2 was obtained.

The solid angle attenuation of the angular distribution, due to the finite dimensions of the detector and source was calculated using a Monte-Carlo program. The corrected angular distribution was found to be

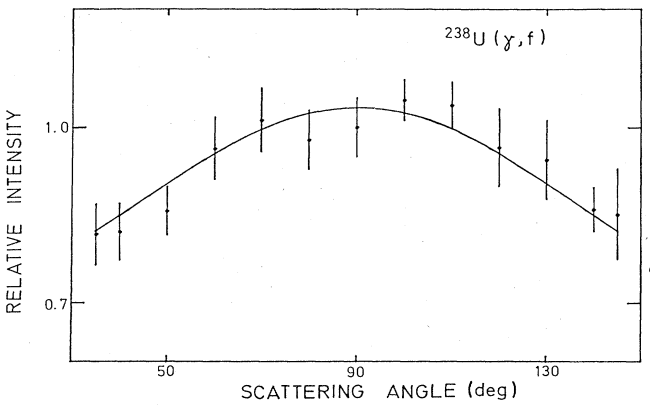

FIG. 1. Angular distribution of the fission fragments. The γ rays were obtained from the Fe(n,γ) source.

$$W(\theta)=1-(0.237\pm0.028)P_2(\cos\theta)\ . \quad (4)$$

B. Measurement of the 249.9 keV line of ^{135}Xe

A second uranium target (depleted to 0.04% ^{235}U), enclosed in a glass vial, consisting of five similar foils, having the same diameter of 1.25 cm and 0.24 g/cm^2 total thickness, was placed at the same geometrical position in the incoming γ beam. The activity of the 249.9 keV ^{135}Xe line was monitored after 47.9 h irradiation in the γ beam, with a Ge(Li) detector of 40 cm^3. One of the spectra taken is presented in Fig. 2. No high fission products activity is present in such a small target even after long irradiations. The 249.9 keV γ line, due to its low energy, has better statistics than other fission products observed in the sample (see the ^{134}I lines at 847 and 884 keV).

The absolute efficiency of the Ge(Li) detector was determined with a calibrated ^{152}Eu source under the same geometrical conditions. The 185 keV γ line, from the decay of ^{235}U present in the target, was used to estimate the self-absorbtion correction factor. Its intensity was measured, before the irradiation, from the five foils of the target beginning with one foil and successively adding the other foils. The effective thickness of the target was extracted, and using gamma attenuation coefficients a self-absorbtion correction factor $g=0.845$ was calculated for the 249 keV line.

Finally, the absolute cumulative yield of ^{135}Xe was found, from Eq. (3), to be 0.0690±0.0047. This is consistent with the value 0.0673±0.0028 obtained by Jacobs *et al.*[1] for the mass chain 135 with a bremsstrahlung beam of 12 MeV end point energy.

IV. MASS DISTRIBUTION

A. Experimental details

For measuring the mass distribution a larger sample was employed in order to obtain measurable counting rates. Thirty grams of U_3O_8 powder, encapsulated in a polyethylene container of about 1 mm wall thickness, were used. This sample was purified of Th and other uranium decay products prior to the irradiation, in order to obtain a cleaner spectrum of fission products after irradiation. It was also necessary to determine the relative efficiency of the detector. The large sample presented a difficult problem for the relative efficiency calibration. We used the ^{234}U γ lines emitted by the sample itself, to calibrate the relative efficiency together with the self-absorption and the geometrical effects. An exponential curve was fitted in the range 250—1200 keV, having an accuracy between 2.5% to 4% at these energies. The relative efficiency curve obtained is presented in Fig. 3.

The integrated incoming photon beam intensity at all energies did not exceed 10^7 photons/cm^2 sec. At these low photon fluxes the experiment was mainly focused on the long-lived fission isotopes (live times between 30 min to a few hours), and the irradiation times were around 15~20 h. The counting was done with a 55 cm^3 Ge(Li) detector in a large lead chamber at the reactor site, ensuring a low background environment. Following the irradiation, up to 27 different 1024 channels spectra were counted, spanning 19 d. The counting times were increased gradually from 1, 2, 3, 8, 24, and 48 h. One of the measured spectra is shown in Fig. 4. The majority of γ rays were identified and assigned to fission isotopes.

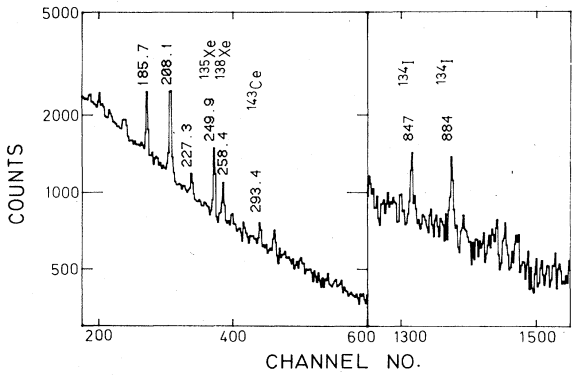

FIG. 2. Spectrum from 0.24 g/cm^2 depleted ^{238}U target, measured after 48 h irradiation, in the beam from the Fe(n,γ) source. Counting time was 130 min, beginning 15 min from the end of the irradiation. Gamma ray energies are in keV (see Sec. III B).

B. Data analysis

To determine fission product yields it was necessary to know: (i) the number n_f of fissions in the sample per unit time (i.e., the flux times the fission cross sections times the number of U nuclei in the target); (ii) the relative efficiency of the detector with respect to the 249 keV line; (iii) the branching ratio B of the measured γ ray, and (iv) the irradiation, cooling, and accumulation times, as well as the half-lives of the parent and daughter. In a parent-daughter-residual (p,d,r) decay chain we have the following differential equations for the number of nuclei:

$$dN_p/dt=-\lambda_p N_p+n_f C_p^c\ ,$$

$$dN_d/dt=-\lambda_d N_d+n_f C_d^i+\lambda_p N_p\ ,$$

where C_p^c is the parent cumulative yield; C_d^i is the daughter independent yield; λ_p,λ_d are decay constants; and n_f is the number of fissions in the target. The same system of equations is true after the end of the irradiation, but of course with $C_p^c=C_d^i=0$.

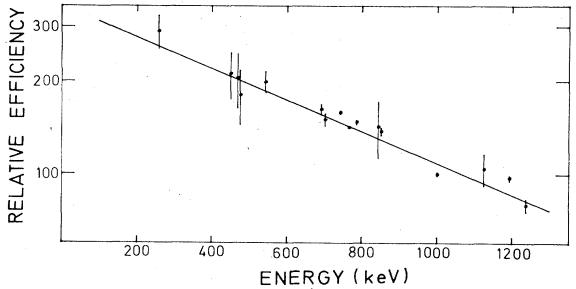

FIG. 3. Relative efficiency calibration of the Ge(Li) detector for the 30 g U_3O_8 target. Use was made of the ^{234}U lines present in the target itself (see Sec. IV A).

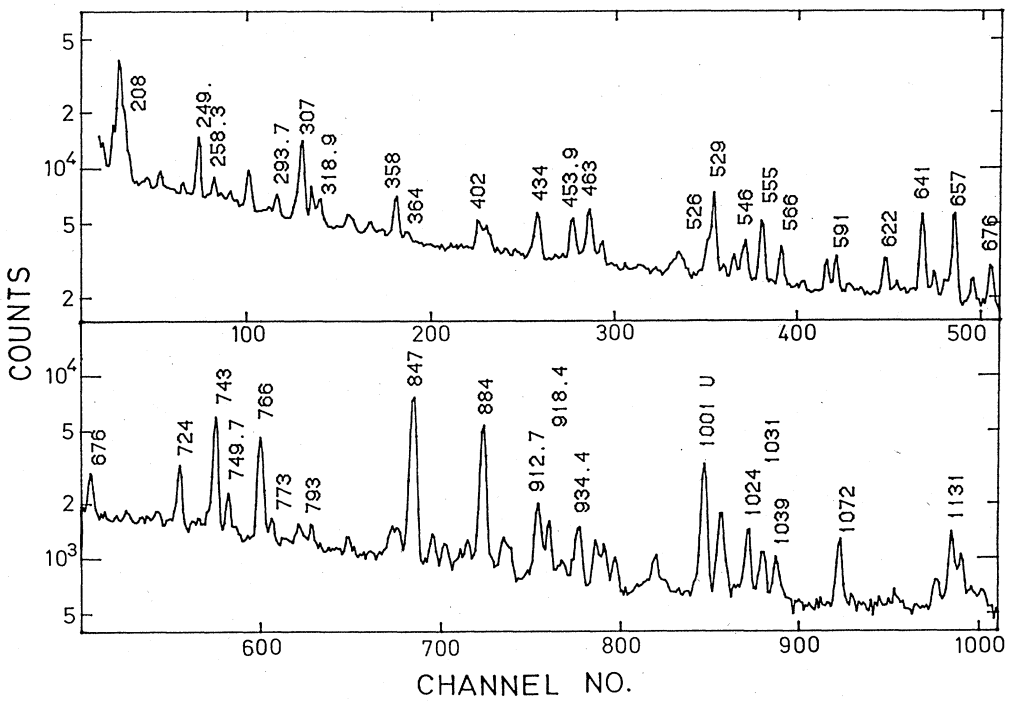

FIG. 4. Spectrum taken from the 30 g U_3O_8 target after 13.6 h irradiation. Counting time was 60 min, beginning 6 min from the end of the irradiation. The γ lines are labeled by their energy in keV.

The general formula for the measured intensity of a daughter γ line in a time interval (t_1,t_2) after the end of the irradiation is given by[9]

$$I_d(T,t_1,t_2)=n_f\epsilon BC_p^c f_p(T,t_1,t_2)+n_f\epsilon BC_d^i f_d(T,t_1,t_2) \tag{5}$$

with the two functions f_p,f_d defined as[9,10]

$$\begin{aligned} f_p(T,t_1,t_2)&=1/(\lambda_d-\lambda_p)\{\lambda_p/\lambda_d[1-\exp(-\lambda_d T)][\exp(-\lambda_d t_2)-\exp(-\lambda_d t_1)] \\ &\quad -\lambda_d/\lambda_p[1-\exp(-\lambda_p T)][\exp(-\lambda_p t_2)-\exp(-\lambda_p t_1)]\}\ , \\ f_d(T,t_1,t_2)&=1/\lambda_d[1-\exp(-\lambda_d T)][\exp(-\lambda_d t_1)-\exp(-\lambda_d t_2)]\ , \end{aligned} \tag{6}$$

where $\epsilon(E_\gamma)$ is absolute efficiency; B is the branching ratio; and T is irradiation time (t_1 and t_2 are measured from the irradiation end).

A linear dependence is obtained for the measured intensity as a function of the ratio f_d/f_p,

$$I_d/f_p=\epsilon Bn_f(C_p^c+C_d^i f_d/f_p)\ . \tag{7}$$

The dependence on n_f was eliminated by measuring all yields with respect to ^{135}Xe, whose absolute cumulative yield C_{135}^c was determined previously;

$$\begin{aligned} I_d/f_p&=(I_d/f_p)^{135}[\epsilon(E_\gamma)/\epsilon(249)](B/B_0) \\ &\quad\times(C_p^c+C_d^i f_d/f_p)/C_{135}^c\ , \end{aligned} \tag{8}$$

when (8) is used, only the relative efficiency curve of the detector is needed (Sec. IV A and Fig. 3). The branching ratios and half-lives were taken from Thierens *et al.*,[10] Blachot and Fiche,[11] and from Dickens and McConnell.[9,12] The data for the first 9 h was thoroughly analyzed. In this period of time the counting rate for most isotopes decreased by one or two orders of magnitude, making their detection in the later spectra very difficult. In Fig. 5 counting rates and the decay of six isotopes are presented.

In the following we will consider three different cases:

$$\begin{aligned} &\text{(I) } \lambda_p \ll \lambda_d \text{ or } T_p^{1/2} \gg T_d^{1/2}\ , \\ &\quad f_d/f_p \sim \lambda_p/\lambda_d \sim 0\ , \\ &\quad I/f_p=\epsilon Bn_f C_p^c\ ; \end{aligned} \tag{9}$$

only the cumulative yield of the parent can be extracted in these cases.

$$\begin{aligned} &\text{(II) } \lambda_p \gg \lambda_d \text{ or } T_p^{1/2} \ll T_d^{1/2}\ , \\ &\quad f_d/f_p \sim 1\ , \\ &\quad I/f_p=\epsilon Bn_f(C_p^c+C_d^i)\ ; \end{aligned} \tag{10}$$

the cumulative yield of the daughter $C_d^c=C_p^c+C_d^i$ is obtained directly in these cases.

(III) $\lambda_p \sim \lambda_d$ or $T_p^{1/2} \sim T_d^{1/2}$.

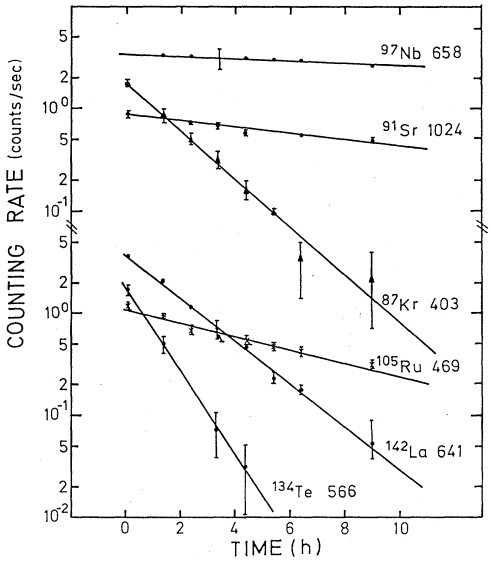

FIG. 5. Counting rates measured for some isotopes from photofission of ^{238}U. A majority of them drop to 0.1 counts/sec after about 10 h.

Most mass chains studied in this work were of type II. For these cases, we obtained the cumulative yield of the daughter $C_p^c + C_d^i$ from relation (8) with $f_d/f_p = 1$. Three chains (i.e., ^{112}Ag, ^{97}Nb, ^{132}I) were of type I, and only the cumulative yield of the parent C_p^c [Eq. (9)] could be deduced in these cases. However, estimates of C_d^i based on the tables of charge distribution of Crouch,[13] show that for these specific isotopes we can safely assume $C_d^i \sim 0$. Finally, for the type III chains we fitted by least squares, the ratio I_d/f_p vs f_d/f_p [Eq. (8)] and obtained both C_p^c and C_d^i. The linear fits are presented in Fig. 6. The method of linear fit was criticized by Dickens and

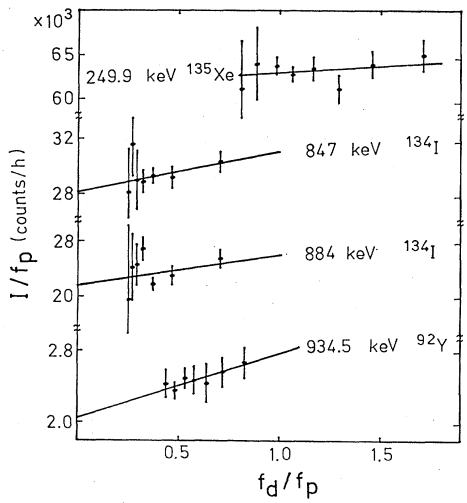

FIG. 6. The measured intensity I/f_p as a function of the dimensionless parameter f_d/f_p for cases requesting type III analysis.

McConnell[9] on the ground that it neglects the uncertainties in f_p and f_d/f_p introduced by uncertainties in the half-lives. We estimated the uncertainties of these factors by random samplings from Gaussian distributions for the half-lives (with standard deviations of 1%). They give an additional 0.5% to 3% uncertainty to be included in our estimates for the ratio $\langle I/f_p \rangle$. This is negligible when summed quadratically with the areas uncertainties.

Table II summarizes the results for all the fission products analyzed in the present experiment. The column denoted by $\langle I/f_p \rangle$ is an average over all the measurements when the analysis was done in the cases I or II. For type III cases the value I/f_p at $f_d/f_p = 1$, extracted from the linear fit, is presented in Table II. The last column of Table II presents the cumulative yields obtained from Eq. (8). The overall uncertainty was estimated by quadratically summing up all the uncertainties in Eq. (8).

Usually, in the decay chain (p,d,r), the measured daughter γ ray is actually a transition in the excited residual nucleus, following the decay of the daughter. There are a few cases in which the daughter has a metastable state and a γ ray is counted from its decay, therefore from the daughter itself. Such a situation is encountered for the 555 keV line of $^{91}Y^m$ or the 305 keV line of $^{85}Kr^m$. Only a fraction b of the β decays of the parent P is feeding the metastable daughter state. Denoting by C_d^i and C_d^{im} the independent yields to the ground state (g.s.) and the excited metastable state, respectively, the decay equations are

$$\begin{aligned} dN_p/dt &= -\lambda_p N_p + n_f C_p^c \ , \\ dN_d^m/dt &= -\lambda_d^m N_d^m + n_f C_d^{im} + b\lambda_p N_p \ , \\ dN_d/dt &= -\lambda_d N_d + n_f C_d^i + \lambda_d^m N_d^m + (1-b)\lambda_p N_p \ . \end{aligned} \tag{11}$$

The second equation above is the one relevant for the metastable state. Its solution has an expression similar to Eqs. (5)—(7) for the measured intensity of a given γ ray, except for the fact that now bf_p appears in place of f_p, and both f_p and f_d are calculated with λ_d^m—the decay constant of the metastable state. It follows that the column $\langle I/f_p \rangle$ in Table II stands for $\langle I/(bf_p) \rangle$ in these cases. The fraction b feeding the metastable state was calculated from the Table of Isotopes,[14] summing all the β-decay branching ratios times the γ decay branching, going directly or indirectly to the metastable state.

The third decay equation appearing in (11) applies particularly to the case of the 249 keV line of ^{135}Xe used by us for normalizing the mass distribution. This isotope has a metastable state at 526.5 keV with a half-life of 15.6 min. It is fed by about 15% of the β decays. The decay of this metastable level to the ground state proceeds via a 526 keV gamma line which can be observed as a shoulder on the 529 keV line of ^{133}I in Fig. 4. The solution of the system above will produce an expression for the integrated intensity I, different from the one presented in Eq. (7). A full expression is given for example by Manohar *et al.*[15] We performed a numerical analysis of the solution, and found, that for irradiation and accumulation times larger than the half-life of the metastable state, and for relatively small values of b (the feeding fraction), the influence of

TABLE II. Principal γ lines and deduced fission products cumulative yields.

E_γ (keV)	Daughter isotope	B (%)	$T_d^{1/2}$ (sec)	$T_p^{1/2}$ (sec)	$\langle I/f_p \rangle$	Relative efficiency	Daughter cumulative yield (%)
228.2	^{132}Te	82.2±0.2	279 720	188	20 735±3715	243.7	2.43±0.50
249.9	^{135}Xe	90±3	32 699	23 796	63 011±3474	237.8	6.90±0.47
258.4	^{138}Xe	31.5±1.3	850	6.5	16 905±2121	235.6	5.38±0.90
293.3	^{143}Ce	43.4±2.0	121 320	840	22 583±196	226.9	5.38±0.62
304.7	^{85}Kr^m	14.6±	16 128	172	984±353	224.4	0.70±0.26[a]
306.9	^{101}Tc	88±4.4	852	877.3	58 579±1525	223.6	6.98±0.82
316.4	^{105}Ru	11.1±0.4	15 984	468	3087±312	221.3	2.95±0.44
316.8	^{146}Ce	52.5±5.7	852	11	16 076±1889	221.2	3.24±0.62
318.9	^{105}Rh	19.2±0.2	127 296	15 984	5153±446	220.7	2.85±0.38
357.9	^{104}Tc	89±5	1080	65.9	33 207±1129	211.5	4.13±0.50
402.6	^{87}Kr	49.5±1.6	4560	55.6	7744±273	201.5	1.82±0.21
453.9	^{146}Pr	48±3	1440	834	14 656±745	190.6	3.24±0.44
462.8	^{138}Cs	30.7±0.6	1932	847.8	15 083±783	188.8	6.10±0.71
469.4	^{105}Ru	18±0.7	15 984	468	4426±279	187.5	3.07±0.39
529.9	^{133}I	87.3±0.2	74 880	3323.9	41 125±610	175.6	6.29±0.65
546.5	^{135}I	8.3±0.4	23 976	18	3526±114	172.4	5.77±0.58
555.6	^{91}Y^m	95.1±0.1	2982.6	34 128	26 631±993	170.7	3.84±0.44[b]
565.9	^{134}Te	18.8±1.0	2508	11	8611±957	168.8	6.36±1.02
617.4	^{112}Ag	42±5	11 304	75 960	529±139	160.2	0.18±0.05[c]
641.3	^{142}La	52.5±2.5	5544	641.9	12 876±200	155.6	3.69±0.43
647.7	^{133}Te*	22.1±2.4	3324	162	3665±307	154.5	2.52±0.43
652.9	^{91}Sr	11.4±	34 128	58	2615±220	153.6	3.50±0.46
657.9	^{97}Nb	98.3±0.1	4326	61 200	33 648±558	152.8	5.25±0.55[c]
667.8	^{132}I	98.7±0.1	8568	279 200	23 834±1652	151.2	3.74±0.46[c]
676.4	^{105}Ru	15.5±0.5	15 984	456	2938±500	150.5	3.03±0.63
724.5	^{105}Ru	48±1	15 984	456	8090±557	142.6	2.77±0.35
743.4	^{97}Zr	97.9±0.3	61 200	1.1	34 253±1387	139.3	5.89±0.66
749.7	^{91}Sr	24.4±	34 128	58	5834±265	138.7	4.04±0.46
767.6	^{134}Te	30.6±1.0	2508	11	10 888±580	136.1	6.13±0.75
773.7	^{131}Te*	38±	108 000	1380	6847±520	135.2	3.12±0.40
812.8	^{129}Sb	45±4.5	15 552	151	1338±165	129.6	0.54±0.10
847.0	^{134}I	95.4±0.3	3156	2508	31 990±3089	124.5	6.31±0.89
884.3	^{134}I	65.3±1.0	3156	2508	20 888±2471	119.6	6.27±0.99
912.7	^{133}Te*	62.8±2.6	3324	150	6777±733	115.9	2.18±0.34
934.5	^{92}Y	13.8±	12 744	9756	2775±453	113.2	4.16±0.21
1024.3	^{91}Sr	33.5±0.7	34 128	58	5717±243	102.7	3.89±0.44
1031.9	^{89}Rb	58±5	912	190	6340±560	101.9	2.51±0.40
1038.8	^{135}I	7.8±0.2	23 796	18	2122±152	101.1	6.31±0.81
1131.0	^{135}I	22.8±0.5	23 796	18	5019±194	91.5	5.64±0.63

[a]A value of $b=1.00$ was used for the fraction feeding the metastable level.
[b]A value of $b=0.59$ was used for the fraction feeding the metastable level.
[c]These are type I chains. Only C_p^c was obtained. We assume $C_p^c \sim C_d^c$ (Sec. IV B).

the metastable state is negligible (less than 0.4% for our experimental conditions) and one can safely use Eqs. (6)—(10). For our measurement of ^{135}Xe the irradiation time was 48 h and therefore, the complications produced by the presence of the metastable state were neglected.

C. Results and discussion

To extract the mass chain yield from the measured cumulative yield of a specific isotope ${}_Z^A X$ in the chain A, an estimate for the fractional independent yield (FIY), for ${}_{Z+1}{}^A X$ was obtained with parameters for the charge distribution from the tables of Crouch,[13] pertinent to fast neutron fission. We found that in all cases the corrections to the cumulative yields due to the direct feeding of ${}_{Z+1}{}^A X$ were less than 1%. The obtained mass distribution is presented in Table III and in Fig. 7. The continuous line is a smoothed curve through the results of Jacobs *et al.*[1] obtained with 12 MeV end point energy bremsstrahlung, which corresponds to 9.7 MeV excitation energy. In Table III we present also results of photofission experiments[1–3] at higher energies.

The mean masses for the light and heavy fragments are

$$m_L = 96.8 \pm 0.2 \text{ and } m_H = 136.6 \pm 0.2 \, . \quad (12)$$

TABLE III. Relative cumulative yields in photofission of ^{238}U. In the present work and in that of Meason and Kuroda (Ref. 14) the γ beam was monoenergetic. For the other quoted works the energy represents the end point of the bremsstrahlung beam.

Mass chain	Present work 7.8 MeV	Jacobs *et al.* (Ref. 1) 12 MeV	Jacobs *et al.* (Ref. 1) 15 MeV	Meason *et al.* (Ref. 14) 17.5 MeV	Jacobs *et al.* (Ref. 1) 20 MeV	Chattopadhyay *et al.* (Ref. 22) 25 MeV
77						0.0673
83				0.24		
84		0.76±0.14	0.90±0.09	0.66	0.84±0.13	
85	0.70±0.26	0.930±0.069	1.09±0.09		1.21±0.09	
87	1.82±0.21	1.87±0.14	2.12±0.16		2.06±0.15	
88		2.27±0.16	2.45±0.12		2.60±0.11	
89	2.51±0.40	3.00±0.18	3.10±0.17		3.01±0.16	
91	3.84±0.31	4.41±0.19	4.39±0.19	4.3	4.30±0.19	4.53
92	4.16±0.21	4.56±0.29	4.78±0.25	4.4	4.80±0.27	4.33
93		4.93±0.43	5.15±0.39		5.02±0.36	4.50
94		5.52±0.40	5.57±0.40		5.33±0.38	
95		5.92±0.25	6.10±0.34		5.70±0.25	5.40
97	5.55±0.42	6.03±0.30	5.82±0.29		5.87±0.29	5.64
99		6.76±0.28	6.13±0.26	5.6	6.17±0.26	5.98
101	6.98±0.82	5.82±0.33	5.71±0.31		5.59±0.30	
103		5.61±0.40	5.14±0.37		4.97±0.37	4.43
104	4.13±0.50	3.69±0.27	3.51±0.26		3.56±0.26	
105	2.91±0.22	2.71±0.28	2.67±0.18	2.5	2.68±0.11	2.61
106		1.74±0.17	1.67±0.23		1.64±0.24	2.39
112	0.18±0.05	0.115±0.022	0.184±0.027		0.311±0.048	0.436
113			0.195±0.040	0.19	0.290±0.039	
115		0.075±0.007	0.172±0.021		0.270±0.025	0.475
117		0.087±0.011	0.171±0.024		0.281±0.031	
123		0.083±0.015	0.176±0.022		0.277±0.034	
127		0.307±0.018	0.533±0.036		0.667±0.0042	0.972
129	0.54±0.10	1.07±0.13	1.38±0.11		1.403±0.092	1.81
131	3.12±0.40	3.73±0.24	4.02±0.26	2.2	3.90±0.24	3.31
132	3.74±0.46	4.95±0.16	4.68±0.31	7.8	4.74±0.39	5.07
133	6.29±0.65	6.80±0.34	6.34±0.37	5.5	6.30±0.35	6.60
134	6.25±0.44	6.88±0.23	6.87±0.25	5.7	6.84±0.22	
135	6.90±0.47	6.73±0.28	6.58±0.29	2.6	6.65±0.28	3.77
137		6.20±0.48	6.13±0.55		6.11±0.55	
138	5.86±0.56					
139				4.9		6.87
140		6.10±0.20	5.91±0.20	6.0	5.59±0.20	5.53
141		5.40±0.38	5.38±0.29		5.05±0.37	6.03
142	3.69±0.43	5.07±0.47	5.02±0.44		4.88±0.37	5.40
143	5.38±0.62	4.80±0.34	4.72±0.34		4.53±0.32	4.51
144		4.60±0.32	4.24±0.46		3.97±0.34	3.18
146	3.24±0.36	3.05±0.22	3.15±0.21		2.90±0.17	

TABLE III. (*Continued*).

Mass chain	Present work 7.8 MeV	Jacobs *et al.* (Ref. 1) 12 MeV	Jacobs *et al.* (Ref. 1) 15 MeV	Meason *et al.* (Ref. 14) 17.5 MeV	Jacobs *et al.* (Ref. 1) 20 MeV	Chattopadhyay *et al.* (Ref. 22) 25 MeV
147		2.40±0.17	2.22±0.15		2.16±0.12	1.78
148						0.77
149		1.36±0.11	1.22±0.15		1.38±0.11	
151		0.792±0.062	0.742±0.067		0.757±0.070	
153		0.300±0.047	0.324±0.053		0.316±0.039	
156						0.029

m_L is in reasonable agreement with the results of Jacobs *et al.*,[1] but m_H is lower by about 1 amu. The discrepancy is due probably to the lack of measured yields on the higher side of the heavy fragments distribution in our experiment.

From Fig. 7 we see that our yields for masses below $A=100$ are consistently lower than those of Jacobs *et al.*,[1] while for $100<A<112$, our values are somewhat larger. This indicates a change in the shape of the light fragments distribution as a function of energy. A similar trend is observed for the heavy fragments although in this case it is less evident because of lack of data for masses beyond $A=146$. This trend is further illustrated in Fig. 8, where some of the yields were plotted versus excitation energy, up to $E_x=15$ MeV. Overall the present work is in good agreement with the results of Jacobs *et al.*[1] at higher energies and follows similar trends as a function of energy.

V. FRACTIONAL CUMULATIVE YIELDS OF ^{92}Sr, ^{134}Te, AND ^{135}I

The fractional cumulative yield FCY(A,Z) of a specific isotope (A,Z) is given by:[13]

$$\mathrm{FCY}(A,Z)=\int_{-\infty}^{Z} N(A)(1+C)(2\pi\sigma^2)^{-1/2} \times\exp\{-\tfrac{1}{2}[Z-Z_p(A)]/\sigma^2\}dz\ , \quad (13)$$

where C is positive for even Z and negative for odd Z, and $N(A)$ is a normalization factor.

The fractional cumulative yields of ^{92}Sr, ^{134}Te, and ^{135}I were obtained from the slope and intercept of I_d/f_p vs f_d/f_p [Eq. (7)], where I_d refers to the γ-line intensity of the respective daughter isotope (i.e., ^{92}Y, ^{134}I, and ^{135}Xe). Experimentally the fractional cumulative yield, FCY, is a relative quantity defined as—$\mathrm{FCY}=C_p^c/(C_p^c+C_d^i)$—and therefore the tedious normalization procedure employed for the absolute yields is not necessary here. The data obtained for these isotopes are presented in Fig. 6 for the

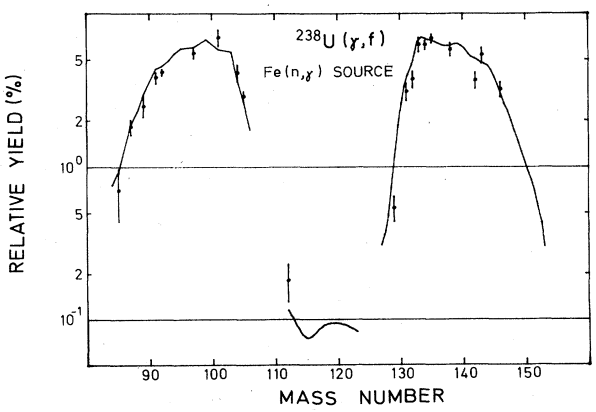

FIG. 7. The fission fragments mass distribution measured in the present experiment. The solid lines are the results of Jacobs *et al.* (Ref. 1) using bremsstrahlung beam with 12 MeV end point energy.

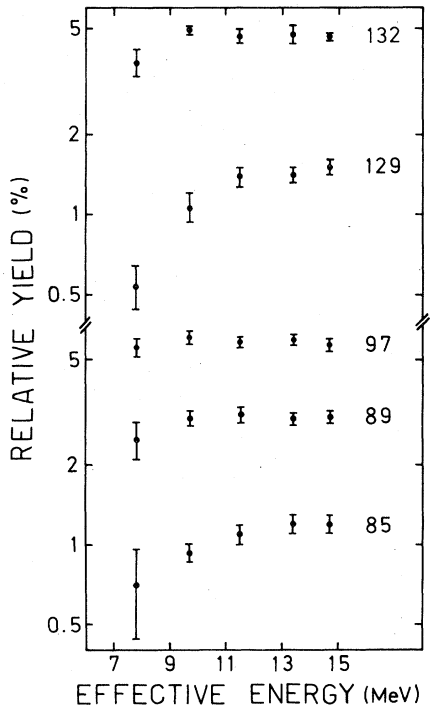

FIG. 8. Cumulative yields for a selected number of mass chains plotted as a function of energy. The points at 7.8 MeV were measured in the present experiment. The higher points were taken from the work of Jacobs *et al.* (Ref. 1) and plotted against the effective energy of the bremsstrahlung beam.

847 and 884 keV lines of ^{134}I, 934.5 keV line of ^{92}Y, and 249.9 keV line of ^{135}Xe. We studied the FCY as a function of energy using three different sources of (n,γ) rays: Fe, Cr, and Ni with average excitation energies of 7.8, 8.8, and 9.0 MeV (Table I). For the Cr source nine spectra of 1 h were measured and for the Ni source only eight, after about 20 h irradiation in each gamma source. These two sets of measurements, together with the previous one from Fe(n,γ) were employed to measure FCY's for ^{92}Sr and ^{135}I. In the case of ^{134}Te we performed a larger number of irradiations (six for the Fe source, six for Cr, and three for Ni) and analyzed 75 spectra, producing more accurate FCY's. The measured FCY's were analyzed in terms of Z_p—the most probable charge of the mass chain, using Table IV (similar to Table III from a recent paper of Dickens and McConnell[16]), in which FCY's are tabulated as a function of a single parameter, Z_p. We calculated this table employing $\sigma=0.61$.[13] Dickens and McConnell's[16] table was calculated with the empirical dependence on Z_p:

$$\sigma(Z_p)=0.62-0.158\cos(\pi Z_p)\ . \tag{14}$$

The difference between the extracted Z_p from our table and from Dickens and McConnell's table, is less than 0.05 charge units, and therefore not relevant.

In fact, two different tables were calculated: one including 25% odd-even effects[13,16] [$C=\pm0.25$ in Eq. (13)], and one without odd-even effects ($C=0$). Our results on FCY's and Z_p's are summarized in Table V.

TABLE IV. Fractional cumulative yields (%) for Z relative to Z_p. The calculations were done for an even value of Z, with a constant charge distribution width of 0.61, and include 25% odd-even effects.

$Z_p=Z+$	$Z-2$	$Z-1$	Z	$Z+1$	$Z+2$
			cumulative yields		
0.00	0.83	15.05	84.95	99.17	100.00
0.04	0.69	13.70	83.51	99.01	100.00
0.08	0.57	12.44	81.97	98.82	100.00
0.12	0.47	11.27	80.34	98.59	100.00
0.16	0.39	10.18	78.61	98.33	100.00
0.20	0.32	9.17	76.77	98.02	99.99
0.24	0.26	8.24	74.84	97.66	99.99
0.28	0.21	7.39	72.81	97.25	99.99
0.32	0.17	6.60	70.68	96.78	99.99
0.36	0.14	5.88	68.46	96.24	99.98
0.40	0.11	5.22	66.14	95.62	99.98
0.44	0.09	4.62	63.74	94.93	99.97
0.48	0.07	4.07	61.26	94.14	99.97
0.52	0.06	3.58	58.71	93.25	99.96
0.56	0.05	3.13	56.10	92.26	99.94
0.60	0.04	2.73	53.43	91.15	99.93
0.64	0.03	2.37	50.72	89.93	99.91
0.68	0.02	2.05	47.98	88.58	99.89
0.72	0.02	1.77	45.23	87.11	99.86
0.76	0.01	1.52	42.48	85.50	99.83
0.80	0.01	1.30	39.74	83.77	99.79
0.84	0.01	1.10	37.03	81.90	99.74
0.88	0.01	0.93	34.36	79.91	99.69
0.92	0.00	0.79	31.76	77.79	99.62
0.96	0.00	0.66	29.23	75.56	99.54
1.00	0.00	0.55	26.79	73.21	99.45
1.04	0.00	0.46	24.44	70.77	99.34
1.08	0.00	0.38	22.21	68.24	99.21
1.12	0.00	0.31	20.09	65.64	99.07
1.16	0.00	0.26	18.10	62.97	98.90
1.20	0.00	0.21	16.23	60.26	98.70
1.24	0.00	0.17	14.50	57.52	98.48
1.28	0.00	0.14	12.89	54.77	98.23
1.32	0.00	0.11	11.42	52.02	97.95
1.36	0.00	0.09	10.07	49.28	97.63
1.40	0.00	0.07	8.85	46.57	97.27
1.44	0.00	0.06	7.74	43.90	96.87
1.48	0.00	0.04	6.75	41.29	96.42
1.52	0.00	0.03	5.86	38.74	95.93
1.56	0.00	0.03	5.07	36.26	95.38
1.60	0.00	0.02	4.38	33.86	94.78
1.64	0.00	0.02	3.76	31.54	94.12
1.68	0.00	0.01	3.22	29.32	93.40
1.72	0.00	0.01	2.75	27.19	92.61
1.76	0.00	0.01	2.34	25.16	91.76
1.80	0.00	0.01	1.98	23.23	90.83
1.84	0.00	0.00	1.67	21.39	89.82
1.88	0.00	0.00	1.41	19.66	88.73
1.92	0.00	0.00	1.18	18.03	87.56
1.96	0.00	0.00	0.99	16.49	86.30
2.00	0.00	0.00	0.83	15.05	84.95

The FCY's obtained for ^{135}I are quite accurate (of the same order as those for ^{134}Te) but, because they lay on the flat wing of FCY as a function of Z_p, the most probable charges extracted have a quite large uncertainty. It

TABLE V. Fractional cumulative yield (FCY), and the most probable charge Z_p for ^{92}Sr, ^{134}Te, and ^{135}I.

	^{92}Sr				^{134}Te			
			Z_p				Z_p	
	E_x	FCY	25% odd-even effects	no odd-even effects	E_x	FCY	25% odd-even effects	no odd-even effects
	7.8	0.60±0.18	38.50±0.29	38.34±0.30	7.8	0.83±0.03	52.06±0.08	51.92±0.07
	8.8	0.73±0.12	38.28±0.24	38.12±0.23	8.8	0.80±0.02	52.12±0.05	51.12±0.04
	9.0	0.76±0.08	38.22±0.17	38.06±0.16	9.0	0.78±0.04	52.18±0.09	52.02±0.08
Average $\langle Z_p \rangle$			38.29±0.12	38.12±0.12			52.12±0.04	51.97±0.03
Waldo *et al.* (Ref. 17)			36.7				51.7	

	^{135}I			
			Z_p	
	E_x	FCY	25% odd-even effects	no odd-even effects
	7.8	0.96±0.08	52.38±0.32	52.44±0.34
	8.8			
	9.0	1.00±0.04	51.12±1.32	51.12±1.32
Average $\langle Z_p \rangle$			52.31±0.31	52.36±0.31
Waldo *et al.* (Ref. 17)			52.15	

should be remarked that the results for ^{135}I FCY's confirm the findings of Okazaki *et al.*,[8] namely that FIY of ^{135}Xe is less than 4%, and therefore the approximation made in Eq. (2) was justified.

From Table V it is clear that for ^{92}Sr and ^{135}I the two sets of Z_p values (with and without odd-even effects) are identical within the errors. For ^{134}Te the values of Z_p obtained without odd-even effects are systematically lower.

The weighted averages of Z_p for all three energies are also given in Table V. These averages are compared with recent formulae obtained by Waldo *et al.*[17] from a systematic analysis of thermal fission of ^{233}U and ^{235}U:

$$Z_p(A<116)=0.4153A-1.19+0.167(236-92A_F/Z_F)\,,$$
$$Z_p(A>116)=0.4153A-3.43+0.243(236-92A_F/Z_f)\,, \quad (15)$$

where $A_F=238$ and $Z_F=92$.

The values of Z_p calculated from these relations are given in Table V. For ^{92}Sr and ^{134}Te the averages of Z_p from our data are considerably larger than the predictions of Eq. (15) (about 10 σ). Even using a larger value of σ in our analysis, does not alter the results significantly. For example, if we use $\sigma=0.8$ in Eq. (13), the averages of Z_p in Table V decrease by about 0.15 charge units. Moreover, the discrepancy persists even when we take into account an energy dependence of Z_p as proposed by Nethaway.[18]

VI. MEASUREMENT OF Γ_n/Γ_f

The ratio of the radiation widths Γ_n/Γ_f is an important parameter in the study of fission. Accurate measurements of Γ_n/Γ_f from photofission are of particular interest in the 5–10 MeV excitation region, where information on the double-humped fission barrier shape can be obtained from this quantity. Measurements of Γ_n/Γ_f from photofission of ^{238}U with neutron capture γ rays were reported until now in two previous experiments[5,18] with about 30% accuracy.

In the present work values of Γ_n/Γ_f were obtained as a by-product of our measurements of the absolute yield of ^{135}Xe. In Fig. 2, besides the 249.9 keV line of ^{135}Xe, a prominent line is apparent at 208.1 keV from the 6.75 d decay of ^{237}U to ^{237}Np. ^{237}U is formed from ^{238}U during the irradiation via the (γ,n) reaction. In the notation of Eq. (2) [i.e., the daughter function f_d, of Eq. (6), is relevant] the measured intensity of the 208 keV line is given by:

$$N_{208}=n_2 I_\gamma \sigma(\gamma,n)\epsilon f_2 B g f_d(T,t_1,t_2)\,, \quad (16)$$

ϵ, B, and g are the values relevant for the 208 line. The ratio $\Gamma_n/\Gamma_f=\sigma(\gamma,n)/\sigma(\gamma,f)$ is calculated by taking the ratio between the activity of the 208 keV line to the fission yield measured with the fission detector [i.e., Eq. (16) to Eq. (1)]. All the experimental parameters appearing in the two expressions were fixed previously in the determination of the absolute yield of ^{135}Xe. The activity of the 208 keV line was measured after the irradiation of the 0.24 g/cm^2 depleted uranium target (0.04% ^{235}U). The depleted target was necessary in order to minimize the ac-

tivity of the 205 keV line of ^{235}U.

The measurement of the Γ_n/Γ_f ratio was done for both Fe(n,γ) and Ni(n,γ) sources. Therefore the fission yield measurement described in Sec. III A was repeated for the Ni source. The obtained angular distribution in this case was almost isotropic. Following a 48 h irradiation, intensities of the 208 keV line were measured in five spectra of 48 h each, up to 10 d. The fission yields were measured in 13 spectra. Values obtained for the Γ_n/Γ_f ratio are

$$\Gamma_n/\Gamma_f = 3.0 \pm 0.3 \text{ at } 7.8 \text{ MeV} ,$$
$$= 3.4 \pm 0.3 \text{ at } 9.0 \text{ MeV} .$$

The major sources of uncertainty are the following: intensity of the 208 keV line (1.5%), fission yield (2.5%), efficiency (3%), and branching ratio (5%). Summing them quadratically and taking into account additional uncertainties due to time and incident beam normalization, number of nuclei in two different targets and self-absorption corrections, an upper limit of 10% is estimated for our accuracy. The above values for the Γ_n/Γ_f ratio are a little higher than those of Mafra *et al.*:[5] 2.3 ± 0.7 and 2.5 ± 0.7 at 7.9 and 9.0 MeV, respectively, but our accuracy is much better. They seem to be in better agreement with Lindner's[19] results. Other values of this ratio found in the literature are the following: 5.0 at 7.8 MeV by Dickey and Axel[20] and about 3.5 at both 8 and 9 MeV by Caldwell *et al.*[7] These two latter results were obtained with bremsstrahlung beams. Our results are also in good agreement with the general systematic trends presented by Vandenbosch and Huizenga,[21] which are obtained from photoneutron and photofission experiments at low energies.

The fission probability P_f could be extracted from the above values of Γ_n/Γ_f via

$$P_f = \Gamma_f/(\Gamma_n+\Gamma_f) = 1-(\Gamma_n/\Gamma_f)/(1+\Gamma_n/\Gamma_f) , \quad (17)$$

producing the values

$$P_f = 0.25 \pm 0.02 \text{ at } 7.8 \text{ MeV} ,$$
$$= 0.23 \pm 0.02 \text{ at } 9.0 \text{ MeV} . \quad (18)$$

These figures are in very good agreement with the fission probabilities in the range 8—12 MeV measured by Caldwell *et al.*[17]

It was shown recently[22] that the experimental values of P_f could be theoretically fitted by accounting for the enhancement of the intrinsic state density due to the deformation of the nuclear shapes at the second fission barrier. The values of P_f in their asymptotic region (i.e., 2—3 MeV above the threshold) are determined by the type of asymmetry assumed at the second fission barrier and by the barrier height. It was definitely shown[22] that a symmetric nuclear shape at the second barrier does not fit the experimental P_f.

For the particular system of ^{238}U, values of P_f around 0.2 and higher support a tentative explanation[23] of fission as a very complex process which approaches simultaneously, two parallel distinct second barriers, one mass asymmetric and the other axially asymmetric but mass symmetric a couple of hundreds of kilovolts higher. The calculated values of P_f obtained assuming only the usual mass asymmetric second saddle, are around 0.1 at 8—9 MeV, much lower than the experimental values given in Eq. (18). It was claimed[22] that at energies >8 MeV the additional axial asymmetric saddle dominates the fission process, thus raising the fission probability to values comparable to our results.

VII. CONCLUSIONS

Highly monoenergetic neutron capture γ rays, at energies lower than 10 MeV, were used to study the fission of ^{238}U. The fission fragments mass distribution was measured and compared with recent results obtained using bremsstrahlung with end points higher than 10 MeV. Values for the most probable charge and fission probability were measured in a few cases. The most probable charges for mass chains 92 and 134 are significantly higher than those predicted by systematics of thermal fission of ^{233}U and ^{235}U. The values of the fission probability support theories assuming a complex structure of the nuclear shapes at the second fission barrier.

[1] E. Jacobs, H. Thierens, D. DeFrenne, A. De Clerq, P. D'hondt, P. De Gelder, and A. J. Deruytter, Phys. Rev. C **19**, 422 (1979).

[2] J. L. Meason and P. K. Kuroda, Phys. Rev. **142**, 691 (1966).

[3] A. Chattopadhyay, K. A. Dost, I. Krajbich, and H. D. Sharma, J. Inorg. Nucl. Chem. **35**, 2621 (1973).

[4] A. Manfredini, L. Fiore, C. Ramorino, H. G. De Carvalho, and W. Wolfli, Nucl. Phys. **A127**, 687 (1969).

[5] O. Y. Mafra, S. Kuniyoshi, and J. Goldemberg, Nucl. Phys. **A186**, 110 (1972).

[6] N. C. Rasmussen, Y. Hukay, T. Inouye, and V. J. Orphan, Air Force Cambridge Research Laboratory, Report No. AFCRL-69-0071, 1969.

[7] T. J. Caldwell, E. J. Dowdy, B. L. Berman, R. A. Alvarez, and P. Mayer, Phys. Rev. C **21**, 1215 (1980).

[8] A. Okazaki, W. H. Walker, and C. B. Bisham, Can. J. Phys. **44**, 237 (1966).

[9] J. K. Dickens and J. W. McConnell, Phys. Rev. C **23**, 331 (1981); see also Ref. 10.

[10] H. Thierens, D. De Frenne, E. Jacobs, A. DeClerq, P. D'hondt, and A. J. Deruytter, Nucl. Instrum. Methods **134**, 299 (1976).

[11] J. Blachot and C. Fiche, At. Data Nucl. Data Tables **20**, 241 (1977).

[12] J. K. Dickens and J. W. McConnell, Phys. Rev. C **24**, 192 (1981).

[13] E. A. C. Crouch, At. Data Nucl. Data Tables **19**, 419 (1977).

[14] *Table of Isotopes*, 7th ed., edited by C. M. Lederer and V. S. Shirley (Wiley, New York, 1978).

[15] S. B. Manohar, T. Data, D. S. Rattan, S. Prakash, and M. V. Ramaniah, Phys. Rev. C **17**, 188 (1978).

[16] J. K. Dickens and J. W. McConnell, Phys. Rev. C **27**, 253 (1983).

[17] R. W. Waldo, R. A. Karam, and R. A. Mayer, Phys. Rev. C **23**, 1113 (1981).

[18] D. R. Nethaway, University of California Radiation Labora-

tory Report No. UCRL-51538, 1974.
[19]M. Lindner, Nucl. Phys. **61**, 17 (1965).
[20]P. A. Dickey and P. Axel, Phys. Rev. Lett. **35**, 501 (1975).
[21]R. Vandenbosch and J. R. Huizenga, *Nuclear Fission* (Academic, New York, 1973), p. 227.
[22]A. Gavron, H. C. Britt, E. Konecny, J. Weber, and J. B. Wilhelmy, Phys. Rev. C **13**, 2374 (1976).
[23]A. Gavron, H. C. Britt, P. D. Goldstone, J. B. Wilhelmy, and S. E. Larsson, Phys. Rev. Lett. **38**, 1457 (1977).